

# Analysis of Coastline Evolution using Landsat and Sentinel 2 Images from 2001 to 2020 in Callao Bay, Peru

Amanda Muñoz<sup>ID</sup><sup>a</sup>, Luis Mendoza<sup>ID</sup><sup>b</sup>, Emanuel Guzmán<sup>ID</sup><sup>c</sup> and Carmela Ramos<sup>ID</sup><sup>d</sup>

Facultad y Escuela de Ingeniería Civil, Universidad Peruana de Ciencias Aplicadas,  
Av. Prolongación Primavera 2390, Santiago de Surco, Lima, Peru

Keywords: Coastal Erosion, Coastal Accretion, Satellite Images, Callao Bay.

**Abstract:** The study presented an analysis of the shoreline evolution in Callao Bay – Lima, Perú; which is one of the most important bays in Perú due to economics and touristic activities. Study areas include La Punta, Callao and Ventanilla districts with an approximate 32 km of length. The study area was divided into six sectors, and the analysis was focused mainly from the 2001 to 2020 period, identifying areas affected by coastal erosion or accretion throughout. Satellite data images were obtained from Landsat (5, 7 and 8) and Sentinel 2, they were processed to correctly identify the shoreline. Shoreline variations were analyzed using the DSAS (Digital Shoreline Analysis System) utility, applying a statistical method called "Linear Regression Ratio". Shoreline variations showed different rates of changes along different sectors of the study area. In general terms, the accretion or erosion trend in Callao Bay was a low accretion with average rates from 3.77 m / year to 4.20 m / year, except in the sector which is closed to the Rímac river with change rate of around 11.85 m/year.

## 1 INTRODUCTION

The constant growth of the population, the flow of economic activities and mismanagement of water use, have directly affected the deterioration of the water resources (Sánchez, 2019). This is directly related to the shoreline, which is of vital importance for the improvement of social, economic, and recreational opportunities; in other words, it is fundamental for the development of the economic and natural environment (Yasir et al., 2020). However, the hazards affecting the coastal zone have increased over the years, resulting from rapid changes in various physical and geological variables that have been influenced by dynamic coastal processes. Likewise, the coastal zone and the water quality has undergone changes due to the influences of anthropogenic activities such as piers and beach protection structures (Sheik Mujabar & Chandrasekar, 2013). This problem is mentioned in a study by Soto (2018), where he highlights how the northern and central coast of Perú has been affected by sediments generated by marine currents and the erosion of river

basins such as the Rímac and Chillón (Soto, 2018). In addition, the metropolitan area of Lima has been affected by constant changes in the shoreline of the Callao Bay (Guzman et al., 2020); specifically in the area near the Callao Port Terminal with a rate of 3m/year between the years 1984 to 2016 (Luijendijk et al., 2018). On the other hand, El Niño, an extreme factor, has a great influence on the displacement of the shoreline in Callao Bay (Guzman et al., 2020).

Therefore, the study of the constant change of the coastline is important so that, based on this, a water resource management strategy can be developed and the negative effects, such as chemical and dynamic imbalance of the coast, loss of coastal biodiversity, and decrease in gross national product (GDP), can be avoided (Rangel-Buitrago et al., 2015). Satellite imagery has been used, to monitor changes along the coastal zone, because it provides repeatable and consistent statistics of variations. In addition, the combination of this methodology with Geographic Information System (GIS) for monitoring the evolution of coastlines on a temporal scale, presents

<sup>a</sup> <https://orcid.org/0000-0002-3512-587X>

<sup>b</sup> <https://orcid.org/0000-0001-7890-9597>

<sup>c</sup> <https://orcid.org/0000-0001-8381-4509>

<sup>d</sup> <https://orcid.org/0000-0002-4269-2944>

a digital structure that facilitates the detection of vulnerable areas (Yasir et al., 2020).

The present study includes the use of Landsat (5,7 and 8) and Sentinel 2 satellite images, to visually identify land and water coverage, also manually obtaining the annual shorelines variations from 2001 to 2020. An analysis of the accretion or erosion tendency of the shoreline will be present through the application of Digital Shoreline Analysis System (DSAS) which is a tool that allows statistical methods such as Linear Regression Ratio (LRR) to be applied to a set of annual coastlines to determine their movement and trends.

## 2 METHODOLOGY

### 2.1 Study Area

Callao Bay is located on the central coast of Perú and belongs to the department of Lima and the Callao Constitutional Province (Figure 1); it also covers La Punta, Callao and Ventanilla districts. Callao Bay is one of the most important bays in Perú due to economics activities that are developed (Callao Port, fishing industry, touristic activities such fishing and water sport). One of the special characteristics of the study area is the presence of the Chillón and Rimac Rivers mouths and Callao port installations.

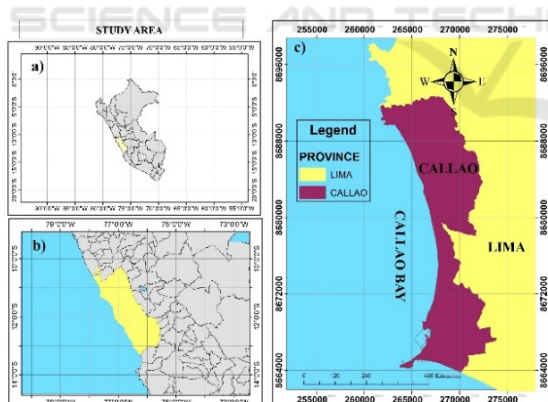


Figure 1: a) Peru, b) Lima and c) Districts covered by the study area.

### 2.2 Data Sources

Images from Landsat and Sentinel 2 satellites were used for the development of the study since they facilitate the remote sensing of the characteristics in the area to be studied. Both satellite image sources are freely available and were obtained from the US

Geological Survey's (USGS) Earth explorer website (<http://earthexplorer.usgs.gov>)

To analyze shoreline variations in study area, one satellite image per year was selected, taking into consideration that an annual coastline was required, and the area shows a constant low tide height with an average of 54 cm per month that was maintained even during the 2017 El Niño phenomenon (DIHIDRONAV, 2020)

The area shows a lot of cloud cover, which made its identification difficult. Therefore, the resolution of the band sets belonging to each satellite were important characteristics to take into consideration (Table 1).

Table 1: Annual satellite image and resolution.

SATELLITE	YEARS	RESOLUTION
Landsat 7	2001, 2002, 2003, 2004, 2012, 2013, 2014 and 2015	Bands 1 to 7 (30 m/pixel) Bands 8 (15 m/pixel)
Landsat 5	2005, 2006, 2007, 2008, 2009, 2010 and 2011	Bands 1 to 7 (30 m/pixel)
Landsat 8	2020	Bands 1 to 7 and 9 (30 m/pixel) Bands 8 (15 m/pixel) Bands 10 and 11 (100 m/pixel)
Sentinel 2	2016, 2017, 2018 and 2019	Bands 1, 9 and 10 (60 m/pixel) Bands 2 to 4 and 8 (10 m/pixel) Bands 5 to 7, 8, 11 and 12 (20 m/pixel)

Therefore Table 2 shows the satellite images, the day they were taken, along with the name and bands that were used.

### 2.3 Image Pre-Processing and Coastline Detection

For this research work, pre-processing steps were applied, using the "Semi-Automatic Classification" plugin of the QGIS program, which simplified the manual extraction of the shoreline.

Table 2: Characteristics of the satellite images used.

YEAR	CHARACTERISTICS OF THE SATELLITE IMAGES USED (2001-2020)				
	SAT.	NAME	DAY	START TIME	BANDS
2001	L7	LT05_L1TP_007068_200 11122_20161209_01_T1	11/22	14:50:15	4, 5, 6 and 7
2002	L7	LE07_L1TP_008068_200 21226_20170127_01_T1	12/26	15:05:15	1, 2, 3, 4, 5,6 and 7
2003	L7	LE07_L1TP_008068_200 30401_20170125_01_T1	04/01	15:05:38	4,5,6,7, and 8
2004	L7	LE07_L1TP_007068_200 40123_20170123_01_T1	01/23	14:59:45	3,4,5,6,7 and 8
2005	L5	LT05_L1TP_008068_200 50430_20161126_01_T1	04/30	15:04:07	5 and 7
2006	L5	LT05_L1TP_008068_200 60503_20161122_01_T1	04/03	15:08:52	5
2007	L5	LT05_L1TP_007068_2007 0328_20161116_01_T1_d	03/28	15:05:50	1, 4, 5 and 7
2008	L5	LT05_L1TP_008068_200 80321_20161101_01_T1	03/21	15:06:48	2, 3, 4, 5 and 7
2009	L5	LT05_L1TP_008068_200 90425_20161026_01_T1	04/25	15:04:18	5 and 7
2010	L5	LT05_L1TP_008068_201 00514_20161015_01_T1	05/14	15:07:42	4, 5 and 7
2011	L5	LT05_L1TP_007068_201 10307_20200823_02_T1	03/7	15:00:40	5, 6 and 7
2012	L7	LE07_L1TP_008068_201 20104_20200909_02_T1	01/04	15:10:56	1, 2, 3, 4,5,6,7 and 8
2013	L7	LE07_L1TP_007068_201 30405_20200907_02_T1	04/05	15:06:47	1, 6, 7 and 8
2014	L7	LE07_L1TP_008068_201 40125_20200906_02_T1	01/25	15:13:41	2, 3, 4, 5, 6 and 7
2015	L7	LE07_L1TP_008068_201 50317_20200905_02_T1	03/17	15:15:54	5, 6, 7 and 8
2016	S2	L1C_T18LTM_A007887_20161225T152814	12/25	15:28:14	2, 3, 4, 8, 11 and 12
2017	S2	L1C_T18LTM_A008416_20170131T152508	01/31	15:25:08	2 and 3
2018	S2	L1C_T18LTM_A004584_20180121T151656	01/21	15:16:56	2, 3, 4 and 8
2019	S2	L1C_T18LTM_A018855_20190131T152414	01/31	15:24:14	2, 3, 4 and 8
2020	L8	LC08_L1TP_007068_202 01126_20210316_02_T1	11/26	15:11:02	1, 2, 6 and 7

### 2.3.1 Image Pre-processing using QGIS

With the QGIS version 3 plugin, the preprocessing was performed to achieve the highest sharpness of the study area comprising the satellite images for the separation of water and land covers from the annual images.

A clip was created for all the bands and the respective atmospheric corrections using the DarkObject Subtraction 1 (DOS1) method (Luca Congedo, 2016), to achieve a complete visualization without noise (visual obstacles in the raster). Subsequently, the combination of bands was performed with different resolutions such as 10m/pixel for Sentinel 2 ,15 m/pixel for Landsat 7 and Landsat 8, and 30m/pixel for Landsat 5. This to achieve a sharper raster that allowed the identification

of the contrast between land and water.

On the other hand, for the years 2004, 2012, 2013 and 2015 only the Landsat 7 satellite image was available, which since 2002 had a banding error due to sensor failure. However, a reliability analysis using a percentage fraction of the parts that are not visible, due to the band error, with the total length of the zone. Led to the conclusion that this failure would not significantly affect the visual identification of the coastline. Figure 2 shows the corrected satellite images for the years between 2001 and 2010 and Figure 3 shows the corrected satellite images for the years between 2011 and 2020.

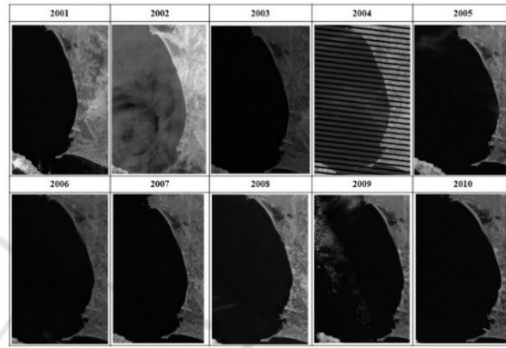


Figure 2: Processed satellite images for years 2001 to 2010.

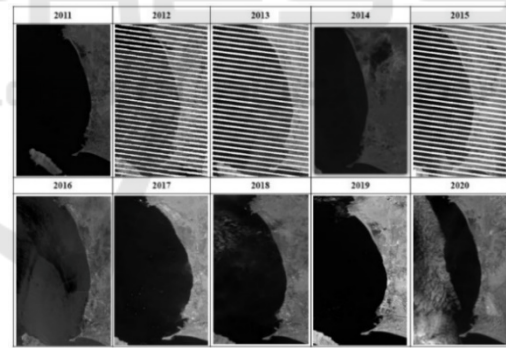


Figure 3: Processed satellite images for years 2011 to 2020.

### 2.3.2 Shoreline Detection

The detection of the shoreline, belonging to the Callao Bay, was performed manually, and validated by importing the polyline into Google Earth where it was georeferenced by date and UTM coordinates. The difference in the range of colors, presented by the satellite images (raster), was considered and in this way the limit between the white pixels (land covers) and black pixels (sea covers) was determined. In addition, the creation of the polyline for the coastline representation was performed with the multiline tool and in the most precise way to avoid taking non-

coastal structures. To perform the analysis, study area was divided into 6 sectors (Figure 4).

The creation of these sectors was made considering the extension of the shoreline; as well as the presence of structures such as the Perú Port Terminal and natural elements such as the mouths of the Rímac and Chillón rivers (Table 3).

## 2.4 DSAS Applications

After collecting the coastlines, belonging to the period 2001 to 2020, with QGIS these were exported in “shape” format to ArcGIS 10.5 and the “Merge” tool was applied to create a single image that would comply all the polylines (20 shorelines). Then, the “Buffer” tool was applied to the compilation of lines to obtain an equidistant margin at 150 meters. Afterwards, geographic database file was created, where two parameters were added for analysis; with names of Coastal Lines and Baseline and were georeferenced in the UTM WGS84 18S zone.

The “Digital Shoreline Analysis System” (DSAS) was used for the analysis of the evolution in the shoreline. Then, the transects were designed with a spacing of 20 meters and a maximum distance from the baseline of 500 meters, considering the sinuosity of the terrain.

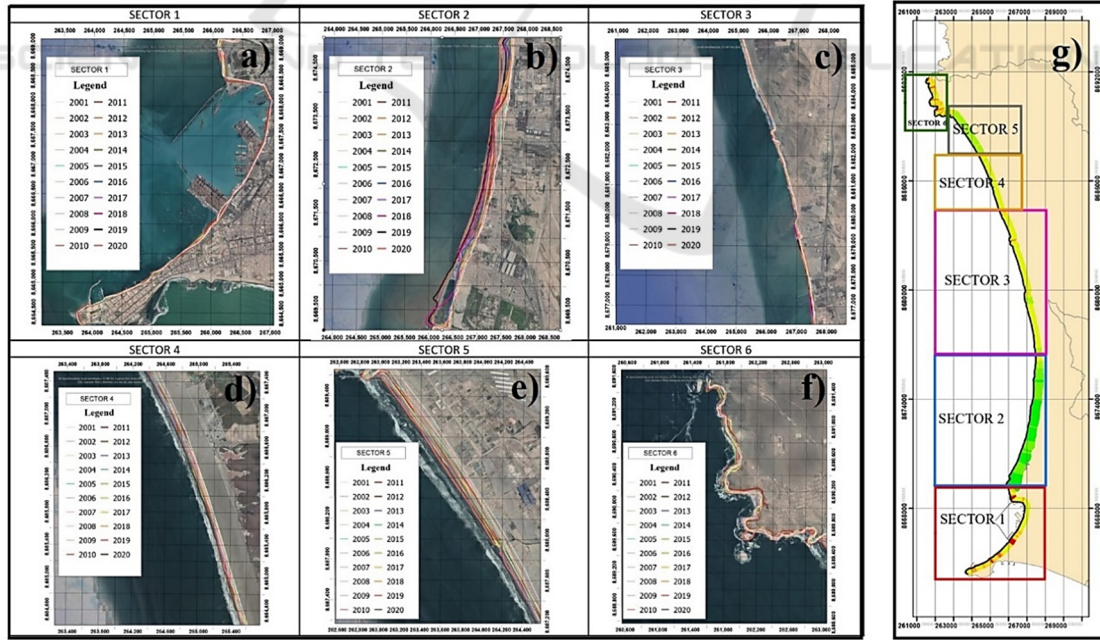


Figure 4: Shorelines from 2001 to 2020 for each sector, a) Sector 1, b) Sector 2, c) Sector 3, d) Sector 4, e) Sector 5, f) Sector 6 and g) Sector Overview.

Table 3: Mainly characteristics of sectors analysis in study area.

Sector	Length (km)	Observations
1	6.95	Presence of the Perú Port Terminal
2	7.18	Rímac mouth is located
3	8.44	Chillón mouth is located
4	3.49	Start zone of Ventanilla's wetlands
5	2.72	End zone of Ventanilla's wetlands
6	3.32	Presence of littoral cliffs

Finally, once the transects were obtained, the data of the intersections between the shorelines and the transects were extracted.

The specified distances indicate how many meters there are between the shorelines of the period and the baseline that was previously created equidistant from the union of the shorelines.

In Figure 5 a map with the transects generated for the shorelines by year and belonging to the period 2001-2020. In this regard, it is important to mention that, although for greater precision the intersection of the transects should be avoided, due to the concave or sinuous shape of the bay, the intersection of the transects could not be totally reduced. However, the few areas where these intersections exist, the close up view 2 of Figure 5, would not be generating a great impact on the analysis for the proposed study.

## 2.5 Statistical Analysis of Shoreline Change Rates

After obtaining the transects, a statistical analysis was performed using LRR method; since one of the advantages of this method is that it considers all the shorelines, thus giving a more detailed analysis (Yasir et al., 2020). For this reason, the DSAS “Calculation of ratios” tool was used, where the rates of change of the shoreline were calculated throughout the 20-year period with the LRR method.

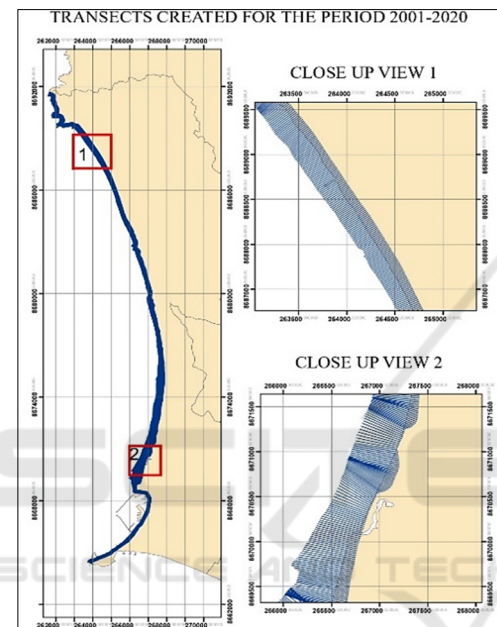


Figure 5: Transects created from the shorelines from 2001 to 2020. In approach 2 it was observed that intersections of the transects that were created due to the sinuousness of the land were created; however, its presence did not significantly affect the calculations performed. Then rates obtained by the LRR method represented with color gamut.

In Figure 6 the different trends for each sector are shown. Likewise, the transects (132 to transect 317) that belonged to the “Terminal Portuario del Perú” were identified, since these transects would not enter the statistical analysis.

To perform the analysis of the variation of the shoreline, the distance data between the shorelines and the baseline extracted from each transect, manually taking 100% of the rates. A subtraction was performed between the total distances of the consecutive years, to then average the data and obtain trends for each sector created.

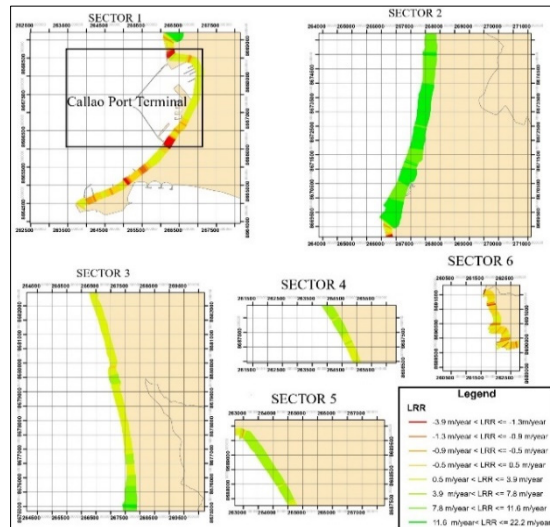


Figure 6: LRR method in the sectorization of the Bay of Callao and detail of sectors.

## 3 RESULTS

Table 4 shows a summary of the average rates of sedimentation, erosion, maximum and minimum, taking 95% of the significant rates. It was identified that some sectors did not show negative erosion data; however, rate trends have been declining over the years.

Table 4: Table of average annual rates by sector applying the DSAS tool (2001-2020).

	From 2001 to 2020					
	Sector 1	Sector 2	Sector 3	Sector 4	Sector 5	Sector 6
Accretion (m/year)	1.53	11.89	2.00	2.47	5.83	0.95
Erosion (m/year)	-1.06	-0.24	-0.44	DP	DP	-0.54
Maximum (m/year)	3.93	22.15	6.19	3.93	7.56	7.18
Minimum (m/year)	-3.85	-0.24	-1.57	0.23	3.62	-2.14
Average (m/year)	0.13	11.85	1.96	2.47	5.83	0.38

Note: DP means "Don't present"

In the same way, a graph was made (Figure 8) of the average historical displacement of the shoreline from 2001 to 2020, which were scaled to achieve a global visualization of the changes per year that have suffered shoreline. Results are described as follows:

- It was observed that sector 1 remains stable, having negative and positive rates of lower value. It was also identified that most of the structures, including springs and the Perú Port Terminal, are in the sector, with a high anthropogenic influence.

- In sectors 2, 4 and 5, an abrupt change was identified that shows high sedimentation between 2016 and 2017, in which the El Niño phenomenon occurred, generating great changes in the natural factors that are present on the coast.
- Sector 3 has shown erosion and sedimentation rates that have increased over the years, with a global tendency to sediment slightly.
- Finally, sector 6, where it is noteworthy to mention, has a large presence of cliffs, showed higher moderate erosion rates, maintaining this trend throughout the 20-year period.

In Figure 7 the displacement of the shoreline in m / year is presented, where the positive value represents sedimentation and the negative value represents erosion, according to the transect number. The highest peak occurs in the sector 2 (transect 349), with a value of 22.15 m / year which is in the northern area of the outlet of the Rímac River and the maximum erosion occurs in sector 1 (transect 322), with a value of -3.85 m / year located in the southern part of the mouth of the Rímac River.

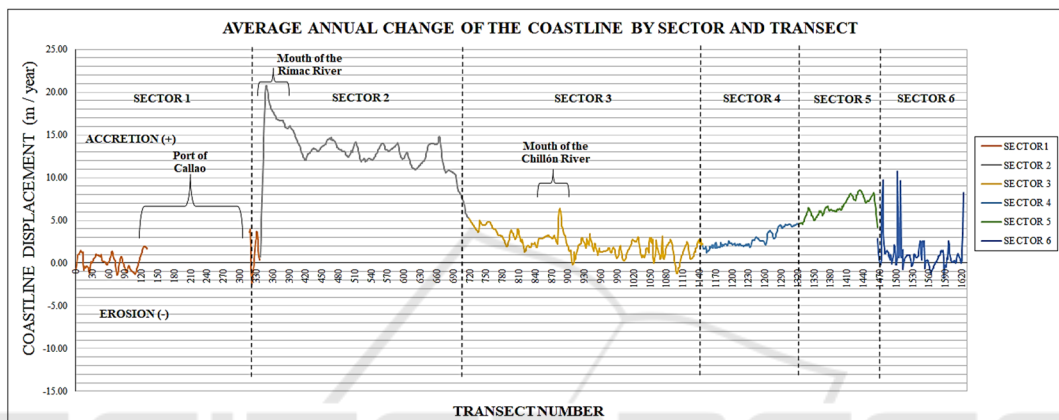


Figure 7: Transects created from shorelines from 2001 to 2020.

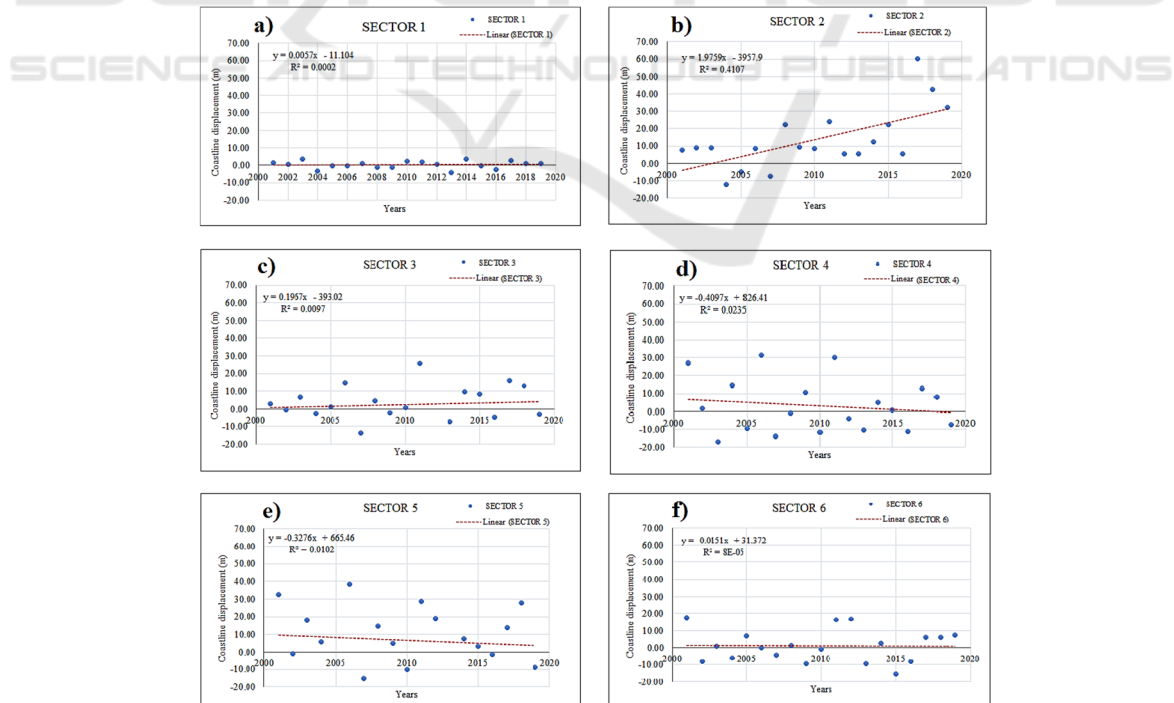


Figure 8: a) Historical analysis by LRR of sector 1, b) Historical analysis by LRR of sector 2, c) Historical analysis by LRR of sector 3, d) Historical analysis by LRR of sector 4, e) Historical analysis by LRR of sector 5, f) Historical analysis by LRR of sector 6.

## 4 DISCUSSIONS

After a comparison with the background of the study presented, it was observed that the tendencies to sediment or erode in some places along the coast of Callao Bay have been maintained despite the presence of extreme factors such as the El Niño phenomenon. As mentioned by Teves and San Román (2012) study, the area between the mouths of the Rímac and Chillón rivers (Sector 2 and Sector 3) has a large presence of sediments that are transported towards the northern part of the mouths due to marine currents (Teves & San Román, 2012). Similarly, the creation of the trend map of the present study showed this accretion between the mouths and the beaches north to the area of the beginning of the cliffs, with a notable increase for the year 2017; however, for subsequent years, sedimentation rates were decreasing minimally.

On the other hand, erosion is a very recurrent process in the surroundings of "Mirador Playa Pachacutec" in sector 6 (Figure 4), this largely due to the steep slopes that occur in the place (Teves & San Román, 2012). The trend map (Figure 8) created shows high erosion rates that are decreasing until showing slight sedimentation rates in certain parts of the sector 6.

In addition, the  $R^2$  factor obtained from the historical analysis (Figure 8), shows a trend to present accretion as it gets closer to 1 and the data present a constant increase, otherwise, while the annual data shows more negative points of erosion, the factor is almost 0.

Likewise, the results obtained from this study have the same sedimentation and coastal erosion trends as Luijendijk's Aquamonitor interface. In this study, the author analyzed the trends of coastlines along the world's continents, showing very general rates of coastal dynamics that could be taken as a base for the present study. (Luijendijk et al., 2018). The comparisons at the total average level are:

- This study shows a sedimentation rate of 0.13m/yr, 11.85m/yr, 1.96m/yr, 2.47m/yr, 5.83m/yr and 0.38m/yr with a difference with the Aquamonitor of 0.26m/yr, 4.50m/yr, 0.37m/yr, -3.31m/yr, -3.09m/yr and -1.00m/yr for sectors 1, 2, 3, 4, 5 and 6 respectively.
- On the one hand, it is worth mentioning that the Aquamonitor presents data from 1984 to 2016 and is a global level study. On the other hand, our study presents data from 2001 to 2020. The differences in rates in sector 2 are mainly due to the occurrence of the 2017 El Niño phenomenon because there was a sediment peak of 60 meters.

## 5 CONCLUSIONS

From the analysis of the sectorization and in general lines of the Callao Bay, it was observed that the trend of the coastline is to present a slight sedimentation with average rates between 3.77 to 4.2 m/year. In addition, sector 2; showed a moderate and constant trend throughout the period that, for the year 2017 suffered an accumulation of sediment that reached up to 60 meters offshore. This is due to the presence of the extreme phenomenon called El Niño, which generated an accumulation of sediment on the beaches located north of the mouths of the Rímac and Chillón rivers.

The temporal analysis shows that sector 1, which includes the Perú Port Terminal, has remained constant when compared to the other sectors. The rates for the 20-year period have had a minimal but progressive increase. Likewise, sectors 2 and 5 have high average sedimentation rates, which have been decreasing in lower values for the last 3 years, since the El Niño phenomenon.

Sector 6 presents high and constant erosion values, due mostly to the presence of cliffs and high slopes in the area; however, the average rate of the sector is to present a slight sedimentation because a large percentage of the rates are positive (Figure 7).

As mentioned above, a Linear Regression Ratio statistical analysis was performed, which was obtained manually and with the application of the DSAS extension. It was observed that both methods show similar trends in the long term. On the one hand, the manual calculation allows to see the annual evolution of changes in average rates, while the DSAS shows an average rate for the 20-year period. In other words, the extension applies statistical methods and takes into consideration the shoreline variations in each confidence interval.

Although the study manages to present erosion or accretion trends for the study area, there is an error range of 5 to 30 meters due to the different resolutions of the satellites used. This affects manual shoreline detection and subsequent statistical analysis. Therefore, the use of higher resolution satellite images or digital elevation models will allow an automatic extraction of the shoreline and, consequently, will improve the extracted data with a smaller error interval than the one presented by the study.

## REFERENCES

- Congedo, L. Semi-Automatic Classification Plugin Documentation (Release 6.0. 1.1). 2016.
- DIHIDRONAV. (2020). Tabla de mareas. Retrieved from <https://www.dhn.mil.pe/portal/tabla-mareas#>.
- Guzman, E., Ramos, C., & Dastgheib, A. (2020). Influence of the el nino phenomenon on shoreline evolution. Case study: Callao bay, Peru. *Journal of Marine Science and Engineering*, 8(2). <https://doi.org/10.3390/jmse8020090>
- Himmelstoss, E. A., Henderson, R. E., Kratzmann, M. G., & Farris, A. S. (2018). Digital Shoreline Analysis System (DSAS) Version 5.0 User Guide. *Open-File Report 2018-1179*, 126.
- Luijendijk, A., Hagenaars, G., Ranasinghe, R., Baart, F., Donchyts, G., & Aarninkhof, S. (2018). The State of the World's Beaches. *Scientific Reports*, 8(1), 1–11. <https://doi.org/10.1038/s41598-018-24630-6>
- Rangel-Buitrago, N. G., Anfuso, G., & Williams, A. T. (2015). Coastal erosion along the Caribbean coast of Colombia: Magnitudes, causes and management. *Ocean and Coastal Management*, 114, 129–144. <https://doi.org/10.1016/j.ocemoaman.2015.06.024>
- Sánchez, L. (2019). *Evaluación De La Calidad Del Agua De Mar En La Playa Cantolao – Sector Espigón Del Abtao En La Bahía Del Callao*. 135.
- Sheik Mujabar, P., & Chandrasekar, N. (2013). Coastal erosion hazard and vulnerability assessment for southern coastal Tamil Nadu of India by using remote sensing and GIS. *Natural Hazards*, 69(3), 1295–1314. <https://doi.org/10.1007/s11069-011-9962-x>
- Soto, R. G. (2018). Dunas y procesos costeros en una isla tropical caribeña amenazada por erosión, actividades humanas y aumento del nivel del mar. *Caribbean Studies*, 46(2), 57–77. <https://doi.org/10.1353/crb.2018.0023>
- Teves, N., & San Román, C. (2012). Geología Marina y Ambiental del litoral limeño entre Ancón y Pucusana. In *XIV Congreso Peruano de Geología*.
- Yasir, M., Sheng, H., Fan, H., Nazir, S., Niang, A. J., Salauddin, M., & Khan, S. (2020). Automatic Coastline Extraction and Changes Analysis Using Remote Sensing and GIS Technology. *IEEE Access*, 8, 180156–180170. <https://doi.org/10.1109/ACCESS.2020.3027881>